

Research Article

High-Temperature Photovoltaic Effect in $\text{La}_{0.4}\text{Ca}_{0.6}\text{MnO}_3/\text{SiO}_x/\text{Si}$ Heterojunction

Hao Ni,^{1,2} Kun Zhao,^{2,3,4} Xiaojin Liu,² Wenfeng Xiang,² Songqing Zhao,² Yu-Chau Kong,³ and Hong-Kuen Wong³

¹ State Key Laboratory of Heavy Oil Processing, China University of Petroleum, Beijing 102249, China

² College of Science, China University of Petroleum, Beijing 102249, China

³ Department of Physics, The Chinese University of Hong Kong, Hong Kong

⁴ International Center for Materials Physics, Chinese Academy of Sciences, Shenyang 110016, China

Correspondence should be addressed to Kun Zhao, zhk@cup.edu.cn

Received 25 November 2011; Accepted 16 January 2012

Academic Editor: Bhushan Sopori

Copyright © 2012 Hao Ni et al. This is an open access article distributed under the Creative Commons Attribution License, which permits unrestricted use, distribution, and reproduction in any medium, provided the original work is properly cited.

We fabricated a heterojunction of $\text{La}_{0.4}\text{Ca}_{0.6}\text{MnO}_3/\text{SiO}_x/n\text{-Si}$ and investigated its electronic transport and ultraviolet photovoltaic properties at higher temperature up to 673 K. The rectifying behaviors vanished with the energy-band structure evolution from 300 to 673 K. Under irradiation of a 248 nm pulse laser, the peak values of open-circuit photovoltage and short-circuit photocurrent decreased drastically. This understanding of the temperature-related current-voltage behavior and ultraviolet photodetection of oxide heterostructures should open a route for devising future microelectronic devices working at high temperature. PACS: 73.40.Lq, 71.27.+a, 73.50.Pz.

1. Introduction

Ultraviolet (UV) sensors have several applications, including flame detection, radiation analysis, drug detection, and environment monitoring. In some cases such as the optical electron sensor for oil and gas optics and the flame detection for a hot engine, thermally stable detectors with high performance are required. Perovskite manganite is a typical system that shows multifunctional properties due to strong electron correlation and magnetic state dependence of the band structure with a chemical stability, which is insensitive to harsh physical environment such as fluctuations of temperature and pressure. Many researchers have devoted time to study the nature of carrier transport in the photoelectric process and explore photoresponse characteristics of devices based on doped manganite thin films and heterostructures [1–8].

Recently, there has been an active study of the photovoltaic properties of the perovskite manganite thin films [9, 10]. Among the different types of detectors, silicon-based photodiode has a great potential for high-temperature detection owing to combine the functional properties of oxides with that of Si electronics [11–13]. In this paper, we aim to develop

an UV photodiode for high-temperature applications, which was fabricated by depositing the $\text{La}_{0.4}\text{Ca}_{0.6}\text{MnO}_3$ (LCMO) thin film on the *n*-type Si (001) wafer. The transport characteristics and UV photodetection were systematically studied in a wide temperature range of 300 to 673 K. The carrier transport and photoresponse properties are discussed with regard to the evolution of band structure by the variation of temperature across the interfaces.

2. Experimental

We fabricated the LCMO/ SiO_x /Si heterojunction by depositing the 100 nm thick LCMO thin film on a native *n*-type Si (001) wafer using facing-target sputtering technique from stoichiometry targets [14]. The two sputtering targets with a nominal composition of LCMO, were prepared using standard ceramic technique. The Si wafer has the carrier concentration of $1 \times 10^{16} \text{ cm}^{-3}$, and a 3 nm thick native silicon oxide layer located on its surface was confirmed by the cross-sectional transmission electron microscopy (TEM) image. During deposition, the substrate temperature was kept

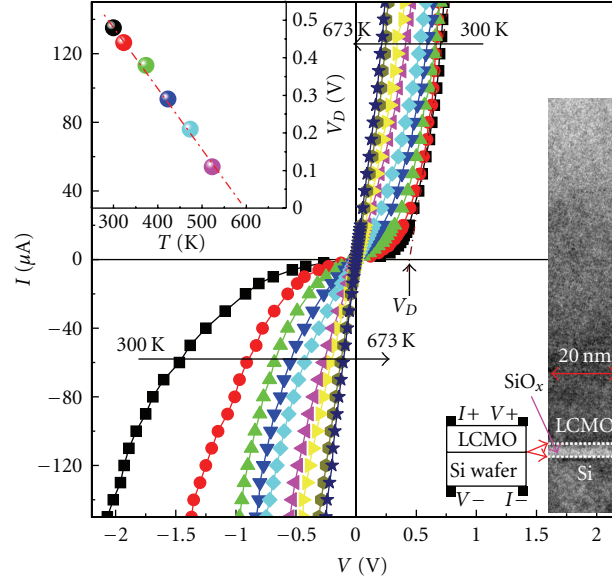


FIGURE 1: The I - V curves of LCMO/SiO_x/Si heterojunction measuring in a wide temperature range from 300 to 673 K. The right inset is the schematic structure of the electrode settings and the cross-sectional TEM image. The left inset shows the diffusion potential V_D as a function of temperature.

at 680°C. The sputtering gas pressure of Ar and O₂ was 60 mTorr with 1:1 gas flow-rate ratio of Ar and O₂. The film thickness was controlled by sputtering time with the deposition rate (~ 0.03 nm/s). After deposition, the vacuum chamber was immediately back-filled with 1 atm oxygen gas to improve the oxygen stoichiometry. And the sample was then cooled to room temperature with the substrate heater power cut-off.

The LCMO/SiO_x/Si sample was 5 mm \times 5 mm in-plane dimension. Before experiments, we carefully cleaned sample using alcohol and acetone. Colloidal silver electrodes of 1 mm \times 5 mm area were printed on the LCMO film and Si substrate. Current-voltage (I - V) characteristics of the junction at different temperatures from 300 to 673 K were measured in a four-probe arrangement using a Keithley 2400. The voltage polarity and the layout of the device are illustrated in the lower inset of Figure 1. A 248 nm KrF pulse laser (20 ns pulse width, 0.15 mJ mm⁻² energy density, and 2 Hz repetition rate) was used to irradiate the LCMO film surface perpendicularly with sample pulse energy of 2.25 mJ. Photovoltaic signals of the sample at different temperatures were recorded with a sampling oscilloscope terminated into 1 M Ω , 50 Ω , and 3 Ω , respectively, as shown in the insets of Figures 2 and 3.

3. Results and Discussion

Figure 1 shows the dark I - V characteristics of the LCMO/SiO_x/Si heterojunction at different temperatures from 300 to 673 K. Electrode settings and the voltage polarity are illustrated schematically in the lower right inset of Figure 1. As can be seen, the heterostructure at room temperature presents a typical rectifying characteristic of a junction diode, which was ascribed to the presence of interfacial potential

obtained from carrier diffusion. The diffusion potential V_D of built-in field in junction can be measured by the voltage at which a current rush occurs in positive bias, and its variation with temperature is presented in the left inset of Figure 1. With the temperature elevating to 673 K, the I - V curves become more and more linear and steeper, and it is nearly linear when temperature was over 523 K. The V_D decreased monotonically with increasing temperature, indicating that accompanied by elevating temperature, the built-in field gradually reduced.

The UV detective property in LCMO/SiO_x/Si heterojunction was measured at different temperatures from 300 to 673 K under a 248 nm laser pulse irradiation. The open-circuit photovoltages (PVs) across the 1 M Ω input impedance of oscilloscope are displayed in Figure 2(a). The PV peak value V_{p1} decreases drastically from 215 to 36.4 mV with increasing temperature from 300 to 673 K as evident shown in the inset of Figure 2(b), and the 10–90% rising time τ_1 of the waveforms decreased from 175 to 25 ns with increasing temperature from 300 to 673 K (inset in Figure 2(b)). We note that the photoresponse is composed of a fast rise time and much slower decay. The RC constant in the circuit should be responsible for the slow decay phenomenon. For the impedance matching, a 50 Ω resistance was connected in parallel with the detector. From the temporal profile of photoresponse waveforms (Figure 2(c)), the PV peak value V_{p2} shows similar tendency as V_{p1} and decreases from 71.7 mV at 300 K to 12.4 mV at 673 K, while the rising time τ_2 drop dramatically and maintains around ~ 17 ns for different temperatures.

For further studying the temperature-dependent photocurrent responses of the LCMO/SiO_x/Si junction, a 3 Ω resistance was connected in parallel with the sample (see the lower left inset of Figure 3). A typical temporal profile of

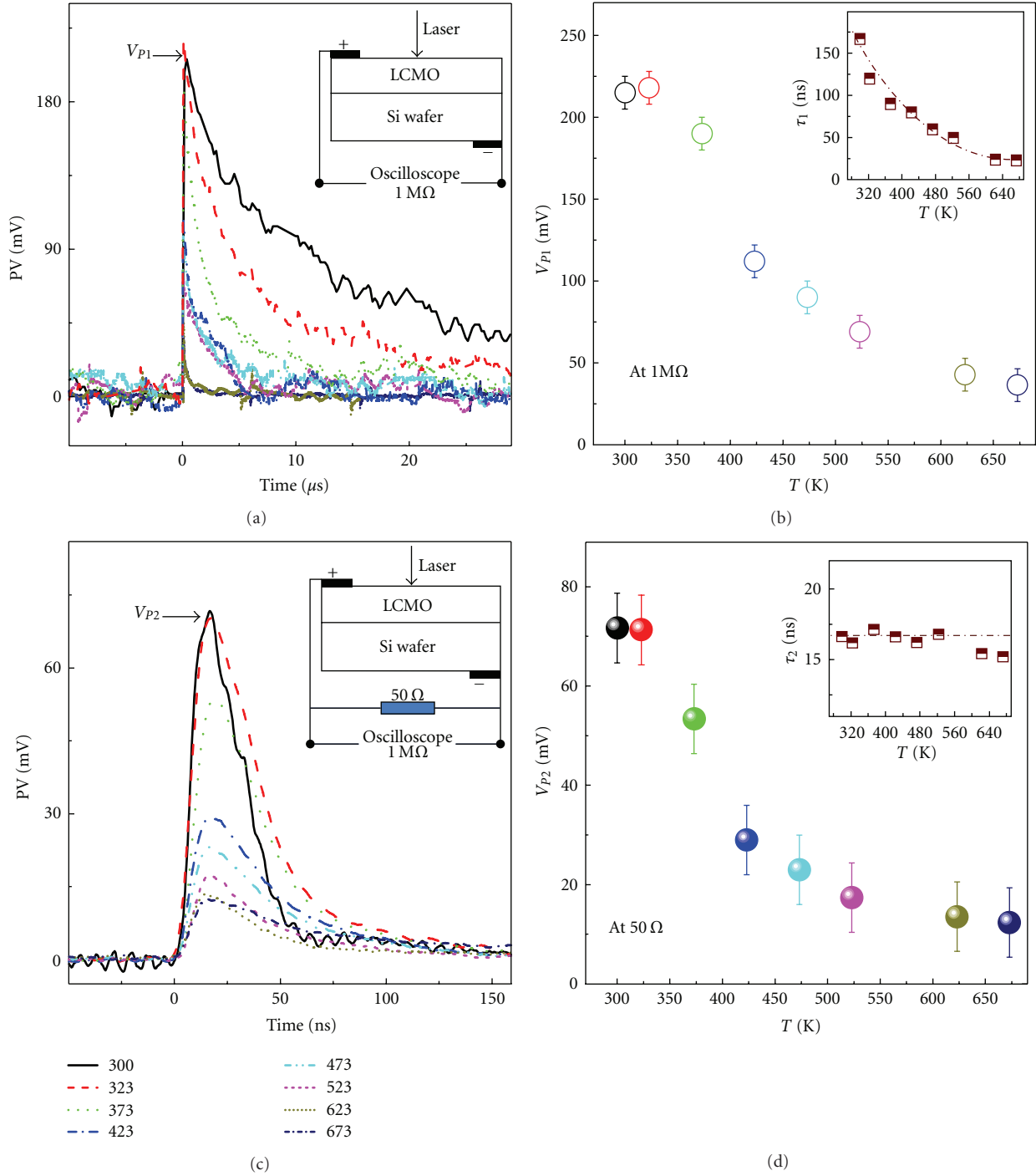


FIGURE 2: Photovoltaic responses for LCMO/SiO_x/Si heterojunction at different temperature from 300 to 673 K under the 248 nm laser illumination recorded by an oscilloscope terminated into (a) 1 MΩ and (c) 50 Ω. The insets of (a) and (c) display the schematic measurement circuits. (b) and (d) present the dependence of PV peak values V_{p1} and V_{p2} on the temperature, respectively. The insets display the temperature dependence of rising time τ_1 and τ_2 of PV pulses shown in (a) and (c).

photoresponse waveforms measured at 523 K is shown in the upper right inset of Figure 3. The peak value V_p and full width at the half maximum (FWHM) are reduced to about 4.3 mV and 7.6 ns, respectively. The peak photocurrent I_p is calculated approximately by $I_p \cong V_p/3\Omega$ where V_p is the

peak voltage across the connected resistance 3 Ω. I_p decreases monotonically to 1.16 mA at 673 K, which is 1.88 times smaller than 3.35 mA at room temperature.

The photon energy of 248 nm wavelength (~ 5.0 eV) is larger than the bandgap (~ 1.2 eV) of LCMO and Si

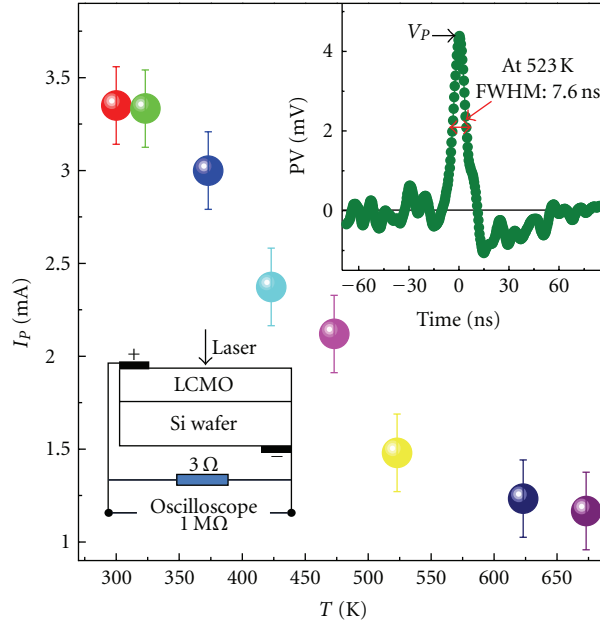


FIGURE 3: The photocurrent peak value I_p as the measurement temperature. The upper inset shows PV pulse at 523 K under 248 nm pulse laser irradiation. The lower inset displays the schematic measurement circuits with a $3\ \Omega$ resistance connected in parallel with the detector.

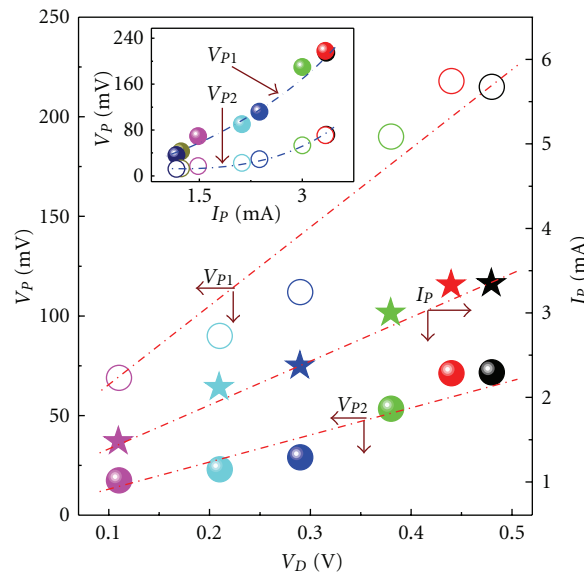


FIGURE 4: Diffusion potential V_D dependences of V_p , V_{p2} , and I_p . The inset shows the relations between V_{p1} , V_{p2} , and I_p .

(~ 1.12 eV). Valence electrons absorb the photons and transit to conduction band, resulting in the photogeneration process of electron-hole pairs. The internal electric field separates the photogenerated electron-hole pairs, leading to photovoltaic responses between two sides of the junction. Based on this understanding, photovoltaic responses would deeply dependent on the built-in field across the junction. The V_p and I_p dependences of diffusion potential V_D are summarized in Figure 4 and V_p increase monotonically with the I_p (inset of Figure 4). We note that the V_p and I_p almost linearly increase with increasing V_D from 0.11 V at 523 K to 0.48 V at 300 K,

indicating that photovoltaic effect due to the built-in field makes the main contribution to the PV signals when the temperature is lower than a certain value (~ 523 K).

At room temperature, the conductivity of LCMO and Si is mainly due to the n -type doping. With increasing temperature, intrinsic excitation gradually becomes the main role in both LCMO and Si, which makes the Fermi level drop down to the middle of band gap. Consequently, the decrease of the built-in field leads to the decrease of the V_D shown in the inset of Figure 1. When the temperature rises to a certain value, the conduction and valence bands in LCMO flush,

respectively, with that in Si, due to near-identical value of band gap in LCMO and Si. The positive bias, driving the intrinsic carriers across the interface potential barrier, has the same value as the negative one. Thus, the I - V curves show symmetry on positive and negative biases at the temperature over 523 K as shown in Figure 1. Meanwhile, due to the higher temperature, hot carriers carry more energy and can be driven over the interface potential barrier induced by SiO_x even by small applied voltage due to Richardson effect. As the temperature continues to rise, hot carriers that carry more energy can freely cross over the potential barrier. Thus, the I - V curves become linear. The experiment results in Figure 1 reflect the evolution of band structure with the increasing temperature.

As mentioned above the 248 nm photons irradiation produces a photovoltage perpendicular to the LCMO/ SiO_x /Si interface because of photovoltaic effect. At room temperature, photoinduced nonequilibrium carriers drift under the built-in electric field within the junction. However, with the increasing temperature, the built-in field becomes weaker and weaker and consequently the diffusion effect plays the main role. So we can see that the peak PVs become smaller with the increasing temperature and then get stabilized.

4. Summary

In conclusion, we fabricated the $\text{La}_{0.4}\text{Ca}_{0.6}\text{MnO}_3/\text{SiO}_x/\text{Si}$ heterojunction and investigated the electronic transport and UV photodetection properties at higher temperature up to 673 K. The I - V curves of the junction change with increasing temperature, which has been explained by considering the energy-band structure evolution at different temperatures. The open-circuit photovoltage and short-circuit photocurrent peak values decreased drastically from 215 to 36.4 mV and 3.35 to 1.16 mA with increasing temperature from 300 to 673 K. The temperature-related UV photodetection properties of oxide heterostructures should open a route for devising future microelectronic devices working at high temperature.

Acknowledgments

This work has been supported by NCET, RFDP, Direct Grant from the Research Grants Council of the Hong Kong Special Administrative Region (Grant no. C001-2060295), and Foresight Fund Program from China University of Petroleum (QZDX-2010-01).

References

- [1] R. Cauro, A. Gilibert, J. P. Contour et al., "Persistent and transient photoconductivity in oxygen-deficient $\text{La}_{2/3}\text{Sr}_{1/3}\text{MnO}_{3-\delta}$ thin films," *Physical Review B*, vol. 63, no. 17, Article ID 174423, 6 pages, 2001.
- [2] H. Katsu, H. Tanaka, and T. Kawai, "Photocarrier injection effect on double exchange ferromagnetism in $(\text{La,Sr})\text{MnO}_3/\text{SrTiO}_3$ heterostructure," *Applied Physics Letters*, vol. 76, no. 22, pp. 3245–3247, 2000.

- [3] M. Rajeswari, C. H. Chen, A. Goyal et al., "Low-frequency optical response in epitaxial thin films of $\text{La}_{0.67}\text{Ca}_{0.33}\text{MnO}_3$ exhibiting colossal magnetoresistance," *Applied Physics Letters*, vol. 68, no. 25, pp. 3555–3557, 1996.
- [4] L. Méchin, J. M. Routoure, B. Guillet et al., "Uncooled bolometer response of a low noise $\text{La}_{2/3}\text{Sr}_{1/3}\text{MnO}_3$ thin film," *Applied Physics Letters*, vol. 87, no. 20, Article ID 204103, pp. 1–3, 2005.
- [5] Y. G. Zhao, J. J. Li, R. Shreekala et al., "Ultrafast laser induced conductive and resistive transients in $\text{La}_{0.7}\text{Ca}_{0.3}\text{MnO}_3$: charge transfer and relaxation dynamics," *Physical Review Letters*, vol. 81, no. 6, pp. 1310–1313, 1998.
- [6] R. D. Averitt, A. I. Lobad, C. Kwon, S. A. Trugman, V. K. Thorsmølle, and A. J. Taylor, "Ultrafast conductivity dynamics in colossal magnetoresistance manganites," *Physical Review Letters*, vol. 87, no. 1, Article ID 017401, 4 pages, 2001.
- [7] N. Takubo, I. Onishi, K. Takubo, T. Mizokawa, and K. Miyano, "Photoinduced metal-to-insulator transition in a manganite thin film," *Physical Review Letters*, vol. 101, no. 17, Article ID 177403, 2008.
- [8] H. Ichikawa, S. Nozawa, T. Sato et al., "Transient photoinduced "hidden" phase in a manganite," *Nature Materials*, vol. 10, no. 2, pp. 101–105, 2011.
- [9] K. Zhao, K. J. Jin, Y. H. Huang et al., "Laser-induced ultrafast photovoltaic effect in $\text{La}_{0.67}\text{Ca}_{0.33}\text{MnO}_3$ films at room temperature," *Physica B*, vol. 373, no. 1, pp. 72–75, 2006.
- [10] X. M. Li, K. Zhao, H. Ni et al., "Voltage tunable photodetecting properties of $\text{La}_{0.4}\text{Ca}_{0.6}\text{MnO}_3$ films grown on miscut LaSrAlO_4 substrates," *Applied Physics Letters*, vol. 97, no. 4, Article ID 044104, 2010.
- [11] H. B. Lu, K. J. Jin, Y. H. Huang et al., "Picosecond photoelectric characteristic in $\text{La}_{0.7}\text{Sr}_{0.3}\text{MnO}_3$ Si p-n junctions," *Applied Physics Letters*, vol. 86, no. 24, Article ID 241915, pp. 1–3, 2005.
- [12] H. Liu, K. Zhao, N. Zhou et al., "Photovoltaic effect in micrometer-thick perovskite-type oxide multilayers on Si substrates," *Applied Physics Letters*, vol. 93, no. 17, Article ID 171911, 2008.
- [13] K. Zhao, K. J. Jin, H. Lu et al., "Transient lateral photovoltaic effect in p-n heterojunctions of $\text{La}_{0.7}\text{Sr}_{0.3}\text{MnO}_3$ and Si," *Applied Physics Letters*, vol. 88, no. 14, Article ID 141914, 2006.
- [14] X. T. Zeng and H. K. Wong, "Epitaxial growth of single-crystal $(\text{La,Ca})\text{MnO}_3$ thin films," *Applied Physics Letters*, vol. 66, no. 3371, 1995.



Hindawi

Submit your manuscripts at
<http://www.hindawi.com>

